Prell, W.L., Wang, P., Blum, P., Rea, D.K., and Clemens, S.C. (Eds.)
Proceedings of the Ocean Drilling Program, Scientific Results Volume 184

Data Report: Pleistocene Paleoclimatic Cyclicity of Southern China: Clay Mineral Evidence Recorded in the South China Sea (ODP Site 1146)[1]

Alain Trentesaux,[2] Zhifei Liu,[3] Christophe Colin,[4]
Sébastien Boulay,[4] and Pinxian Wang[3]

ABSTRACT

The preliminary results of a comprehensive study of clay minerals (<2 µm) are presented for the upper 2 m.y. of sediments from Ocean Drilling Program Leg 184 Site 1146 from the northern margin of the South China Sea, close to the Pearl River mouth. More than 500 samples were analyzed, and four main mineral species are present: smectite, illite, chlorite, and kaolinite. On a general basis, illite + chlorite and smectite display anti-correlated behavior in relation to changes in the proportion of primary to secondary minerals in the sediment. Low-frequency and high-frequency changes are observed in the smectite/(illite+chlorite) ratio.

INTRODUCTION

The South China Sea (SCS) is one of the marginal seas found in the western Pacific Ocean. Sediments typically consist of terrigenous material, biogenic carbonates, and opal, as well as small amounts of volcanic material. The sea is mainly fed by discharges from the Mekong, Red, and Pearl Rivers. However, during past glacial stages, the paleo-Sunda River system may have contributed large amounts of sediment to the

[1] Trentesaux, A., Liu, Z., Colin, C., Boulay, S., and Wang, P., 2003. Data report: Pleistocene paleoclimatic cyclicity of southern China: clay mineral evidence recorded in the South China Sea (ODP Site 1146). *In* Prell, W.L., Wang, P., Blum, P., Rea, D.K., and Clemens, S.C. (Eds.), *Proc. ODP, Sci. Results,* 184, 1–10 [Online]. Available from World Wide Web: <http://www-odp.tamu.edu/publications/184_SR/VOLUME/CHAPTERS/210.PDF>. [Cited YYYY-MM-DD]
[2] UMR PBDS du CNRS, FR 1818. Université des Sciences et Technologies de Lille SN5, 59655 Villeneuve d'Ascq Cedex, France. **Alain.trentesaux@univ-lille1.fr**
[3] Laboratory of Marine Geology, MOE, Tongji University, 1239 Siping Road, Shanghai 200092, People's Republic of China.
[4] Géochimie des Roches Sédimentaires, UMR CNRS-UPS Orsayterre, Université de Paris-Sud., Bat 504, 91405 Orsay Cedex, France.

Initial receipt: 12 September 2001
Acceptance: 19 December 2002
Web publication: 16 May 2003
Ms 184SR-210

SCS (Shipboard Scientific Party, 2000). Our objective is to study the detrital input to hemipelagic sedimentation during the Pleistocene using clay minerals as tracers.

Clay minerals are thought to change through time because of climate modifications (Windom, 1976; Bouquillon et al., 1990; France-Lanord et al., 1993). Specifically, smectite, mixed-layer clay minerals, and kaolinite could be produced under high hydrolysis regimes in soils, whereas illite and chlorite are produced by physical erosion of igneous and other rocks. If these statements are correct on a long-term basis, very rapid changes in clay mineral content, such as those observed during the Pleistocene, cannot be a result of similarly rapid changes in hydrolysis conditions; instead, clay mineral assemblages could reflect changes in the sedimentation/erosion balance on the continent. Therefore, sea level changes could have caused a very efficient redistribution of clay minerals from the continent or shelf to the ocean.

During the Pleistocene, the Asian continent experienced many changes, especially because of glacial–interglacial climate oscillations. These changes in climate conditions could also have altered either the intensity or seasonality of the Asian monsoon. Such changes are likely to have been recorded in the sediments through their finest component, the clay minerals. While the history of the East Asian monsoon has been well studied from sediments of the Chinese loess plateau using different proxies such as grain size or clay minerals (An et al., 1990; Chen et al., 1997; Lu et al., 2000), very few similar studies of SCS sediments have been undertaken (Wang et al., 1999). Clay minerals are very sensitive to the inland hydrolysis regime. Our objective is to use the mineralogical-assemblage inclinations as tracers of the climactic changes.

The size of the exposed continental shelf has varied considerably during such climatic oscillations on similar timescales. Site 1146 is located ~400 km offshore from Hong Kong and the Pearl River mouth, at 2092 m water depth. At this location, 200 km separates the shore from the –100-m isobath contour line (Fig. **F1**). Accordingly, the drainage basin area of the Pearl River (and limited coastal rivers flowing into the SCS between the Hainan and Taiwan Islands) would have increased by ~45% when the sea level was located at around –100 m during glacial maxima.

F1. Location of Site 1146 and major drainage systems, p. 7.

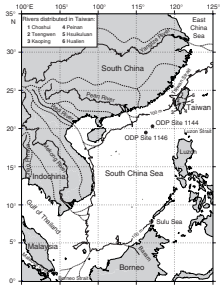

MATERIALS AND METHODS

Core

During Ocean Drilling Program (ODP) Leg 184, a series of six sites was drilled in the South China Sea. Among them, Site 1146, located within a small rift basin on the midcontinental slope of the northern SCS (Fig. **F1**), was cored with a maximum penetration of 633 meters below seafloor (mbsf). This core contains hemipelagic sediments dating from the early Miocene to the Pleistocene. For this study, our analysis concentrated on the latest 2 m.y., corresponding to the upper 190 meters composite depth (mcd). The sediment is relatively homogeneous and consists of greenish gray nannofossil clay with an average of ~21 wt% carbonate content, and the age model was established using paleontological and magnetic data (Shipboard Scientific Party, 2000).

Methods

Clay mineralogy determination was performed by standard X-ray diffraction (XRD) on a set of 508 samples on the composite splice from Site 1146 from Holes 1146A, 1146B, and 1146C. According to the preliminary sedimentation rate calculated onboard and in order to keep an average sampling interval of 4 k.y., the sampling interval was averaged to 40 cm, reducing with decreasing sedimentation rate downcore. An extra set of 181 samples was later collected from the upper 60 m for refining the latest intervals. All samples were disaggregated in water and treated with 0.2-N hydrochloric acid to remove carbonates. During this operation, the suspension was kept agitated and the pH checked to avoid irregular or prolonged exposure to the acid. The decarbonated suspensions were washed with demineralized water to remove excess ions and to help disperse the clays. Stoke's Law was applied for the determination of settling time and depth to isolate the <2-µm size fraction. The clay fraction was concentrated in a centrifuge, and the resulting paste was spread into a calibrated recess cut into rounded glass slides.

Preparation and measurement were performed according to the routine procedures of Holtzapffel (1985). Briefly, a Philips PW 1710 diffractometer equipped with a Cu tube and Ni monochromator was used with the following settings: 40 kV, 25-mA generator tension/current, 1° fixed divergence slit, 0.1° receiving slit, with sample spinner on. All samples were scanned three times in step-scan mode with 1 s per step of 0.02°2θ: (1) air-dried, (2) glycolated (12 hr under vacuum in ethylene glycol at room temperature), and (3) heated (2 hr at 490°C) from 2.5° to 32.5°2θ.

The diffractometer is driven by a computer that gives peak intensities for each 0.02°2θ interval. The spectra were then studied using the MacDiff software (Petschick, 1997). We used the peak surface calculated by the software as an indicator of clay-mineral amount. We realize that this technique does not permit the production of fully quantitative results, but rather results in semiquantitative mineral percentages. Repeated measurements indicate that replicates of the same sample give very similar results and that peak ratio calculations are very stable, thus lowering the uncertainties resulting from preparation and analysis. Measurements have been carried out on the basal reflections from the ethylene glycol XRD diagram, adjusted on the 4.26-Å quartz peak.

RESULTS

XRD diagrams display different minerals including quartz and feldspars. Clay minerals mainly consist of chlorite, illite, smectite, and kaolinite (Fig. F2). Analyses indicate that illite-smectite mixed layers are also present in small amounts. We decided to combine the smectite and illite-smectite mixed-layer content, since in detail, these two minerals vary with the same trends and are sometimes hard to distinguish on the diagrams. Mixed-layer clay minerals slightly enlarge the glycolated peak of smectite at 17 Å. Smectite-illite mixed layers correspond to randomly mixed-layered clays. Combining these two species as "smectite" follows naturally, as some studies have shown a very similar behavior of these phases and smectite is sometimes considered as a special case of illite-smectite mixed layers (see numerous examples, e.g., Chamley, 1989). For the rest of this study, we group these minerals under the generic

F2. XRD diagrams, p. 8.

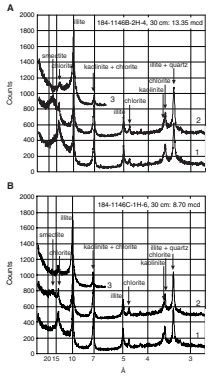

term of "smectite." Kaolinite and chlorite are the less abundant species, with an average content of 2%–18% and 10%–30%, respectively (Fig. F3; Table T1). In contrast, illite and smectite are more abundant and represent 22%–43% and 30%–55% of the clay fraction, respectively. These sediments are, on average, slightly enriched in smectite compared to equivalent sediments studied from Site 1144 (Fig. F1) (Boulay et al., this volume). Chlorite and illite display similar behavior with in-phase peaks, whereas illite and smectite display antiphase behavior indicative of a change in the clay mineral input. The opposition between smectite and illite + chlorite is especially well expressed below 110 mcd but is also visible in the upper part of this section. The last mineral, kaolinite, does not seem to vary in phase with any of the other minerals and exhibits a relatively stable average abundance of 12%.

F3. L* and clay-mineral assemblages, p. 9.

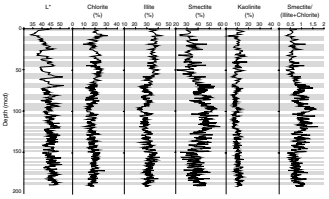

T1. Depth and relative abundance of clay-mineral constituents, p. 10.

PRELIMINARY OBSERVATIONS

Overall, two groups of clay minerals display opposite behavior. Illite and chlorite mainly derive from the degradation of micas (biotite and muscovite) from igneous, metamorphic, or sedimentary rocks (Chamley, 1989). These two minerals are, therefore, considered as primary minerals, derived from physical erosion or weak chemical weathering. On the contrary, both smectite and kaolinite are formed by the hydrolysis of primary minerals in the soils. These soils are located in the lowermost parts of the Pearl River drainage basin, where soils can develop and produce secondary minerals. In response to the climatic changes described earlier, it is likely that the mineral composition will have changed because of the physical/chemical weathering balance. Since kaolinite is present only in low amounts, we focus our clay-mineral analysis on the smectite/(illite+chlorite) ratio. This ratio is compared with the L* index (Fig. F3), representing the sediment lightness (Blum, 1997; Balsam et al., 1999). This parameter typically increases with increasing calcium carbonate content and therefore could be a proxy for either elevated calcium carbonate production or reduced input of the detrital fraction. According to the preliminary age model (Shipboard Scientific Party, 2000), predominantly lighter intervals coincide with interglacial stages.

On a long-term basis, smectite exhibits a three-step behavior, with an increase between 1200 and 400 ka. During this interval, chlorite and illite decrease relatively, whereas the abundance of kaolinite appears to remain stable. At higher temporal frequency, smectite/(illite+chlorite) display large variations throughout the core, most of them being associated with changes in L*.

CONCLUSION

The study of the clay content of >500 samples covering ~2 m.y. from Site 1146, located in the northern part of the SCS, indicates that clay-mineral content varies widely with different frequency orders. A refined age-model is needed to study the mechanisms that drive these changes.

ACKNOWLEDGMENTS

The authors are pleased to thank the French-Chinese program under the NR AFCRST PRA 99-02. This program allowed Z. Liu to visit France as a postdoctoral researcher during which he performed most of the clay analyses. This research used samples provided by the Ocean Drilling Program (ODP). ODP is sponsored by the U.S. National Science Foundation (NSF) and participating countries under management of Joint Oceanographic Institutions (JOI), Inc. Funding for this research was provided by the French "Océans" Program of INSU that helped us in performing the analyses and the French committee of ODP. P. Recourt and D. Malengros are warmly thanked for their technical assistance in the laboratory. We thank Matthew Higginson for his patient and thorough editing of a draft of this manuscript. The authors gratefully acknowledge G.J. Reichart, D.C. Leuschner, and L. Krissek and the Senior Publications Coordinator G. Delgado for her thorough review.

REFERENCES

An, Z., Liu, T., Lu, Y., Porter, S.C., Kukla, G., Wu, X., and Hua, Y., 1990. The long-term paleomonsoon variation recorded by the loess-paleosol sequence in central China. *Quat. Int.,* 8:91–95.

Balsam, W.L., Deaton, B.C., and Damuth, J.E., 1999. Evaluating optical lightness as a proxy for carbonate content in marine sediment cores. *Mar. Geol.,* 161:141–153.

Blum, P., 1997. Physical properties handbook: a guide to the shipboard measurement of physical properties of deep-sea cores. *ODP Tech. Note,* 26 [Online]. Available from World Wide Web: <http://www-odp.tamu.edu/publications/tnotes/tn26/INDEX.HTM>. [Cited 2003-03-05]

Bouquillon, A., France-Lanord, C., Michard, A., and Tiercelin, J.-J., 1990. Sedimentology and isotopic chemistry of the Bengal Fan sediments: the denudation of the Himalaya. *In* Cochran, J.R., Stow, D.A.V., et al., *Proc. ODP, Sci. Results,* 116: College Station, TX (Ocean Drilling Program), 43–58.

Chamley, H., 1989. *Clay Sedimentology:* Berlin (Springer-Verlag).

Chen, F.H., Bloemendal, J., Wang, J.M., Li, J.J., and Oldfield, F., 1997. High-resolution multi-proxy climate records from Chinese loess: evidence for rapid climatic changes over the last 75 kyr. *Palaeogeogr., Palaeoclimatol., Palaeoecol.,* 130:323–335.

France-Lanord, C., Derry, L., and Michard, A., 1993. Evolution of the Himalaya since Miocene times: isotopic and sedimentological evidence from the Bengal Fan. *In* Treloar, P.J., and Searle, M. (Eds.), *Himalayan Tectonics*. Spec. Publ.—Geol. Soc. London, 7:603–621.

Hiscott, R.N., 2001. Depositional sequences controlled by high rates of sediment supply, sea-level variations, and growth faulting: the Quaternary Baram Delta of northwestern Borneo. *Mar. Geol.,* 175:67–102.

Holtzapffel, T., 1985. Les minéraux argileux: préparation, analyse diffractométrique et détermination. *Publ. Soc. Geol. Nord.,* 12.

Lu, H., van Huissteden, K., Zhou, J., Vandenberghe, J., Liu, X., and An, Z., 2000. Variability of East Asian winter monsoon in Quaternary climatic extremes in North China. *Quat. Res.,* 54:321–327.

Petschick, R., 1997. Powder Diffraction Software. *MacDiff* [Online]. Available from World Wide Web: <http://www.servermac.geologie.uni-frankfurt.de/Staff/Homepages/Petschick/RainerE.html>. [Cited 2003-03-05]

Shipboard Scientific Party, 2000. Site 1146. *In* Wang, P., Prell, W.L., Blum, P., et al., *Proc. ODP, Init. Repts.,* 184, 1–101 [CD-ROM]. Available from: Ocean Drilling Program, Texas A&M University, College Station TX 77845-9547, USA.

Wang, L., Sarnthein, M., Erlenkeuser, H., Grimalt, J., Grootes, P., Heilig, S., Ivanova, E., Kienast, M., Pelejero, C., and Pflaumann, U., 1999. East Asian monsoon climate during the late Pleistocene: high-resolution sediment records from the South China Sea. *Mar. Geol.,* 156:245–284.

Windom, H., 1976. Lithogenous material in marine sediments. *In* Riley, J.P., and Chester, R. (Eds.), *Chemical Oceanography* (Vol. 5): New York (Academic Press), 103–135.

Figure F1. Location of Site 1146 in the South China Sea and major drainage systems. The thick line offshore corresponds to the present 100-m isobath, approximating the lowest sea level during glacial maxima. The location of the major rivers on the emerged glacial shelf, corresponding to paleorivers, are adapted from Wang et al. (1999) and Hiscott (2001).

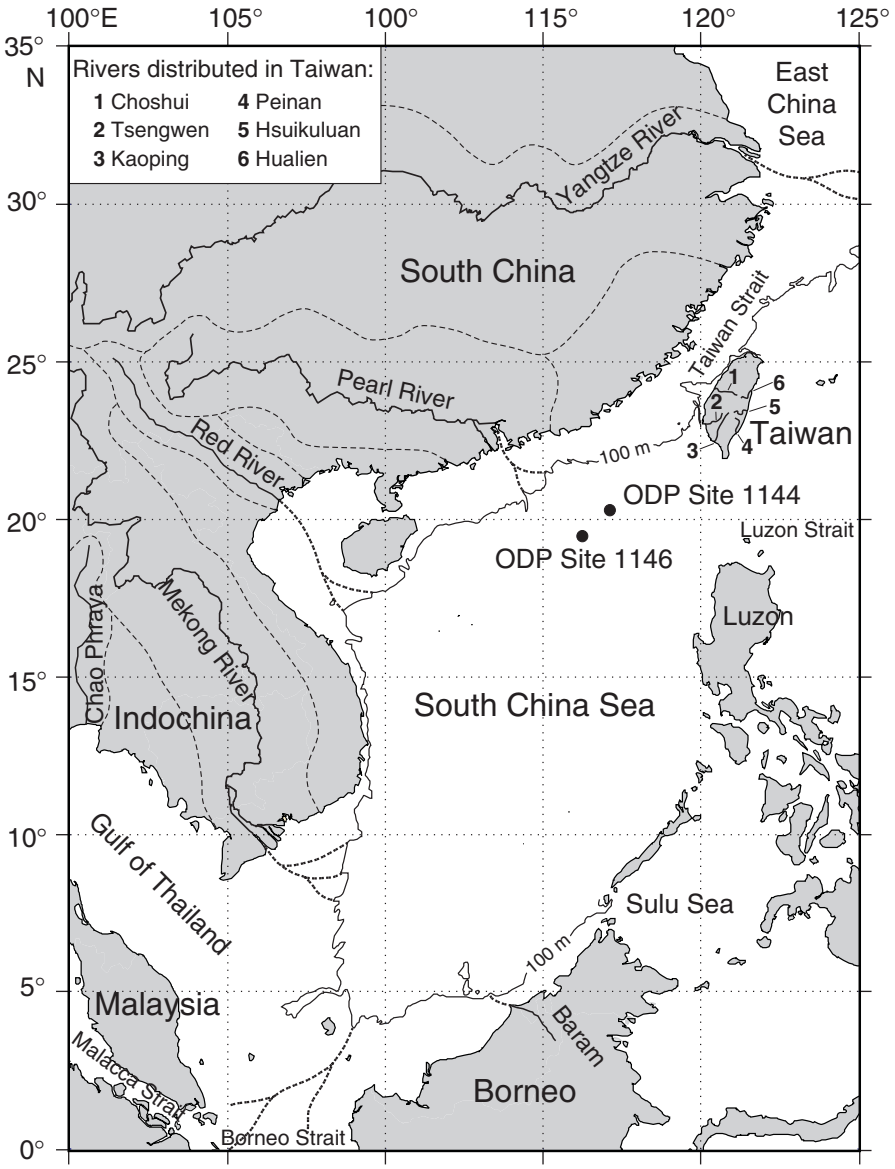

Figure F2. Typical XRD diagrams showing (**A**) smectite-type rich (relative to illite) and (**B**) smectite-type poor samples. The three curves represent (1) normal, (2) glycolated, and (3) heated diagrams.

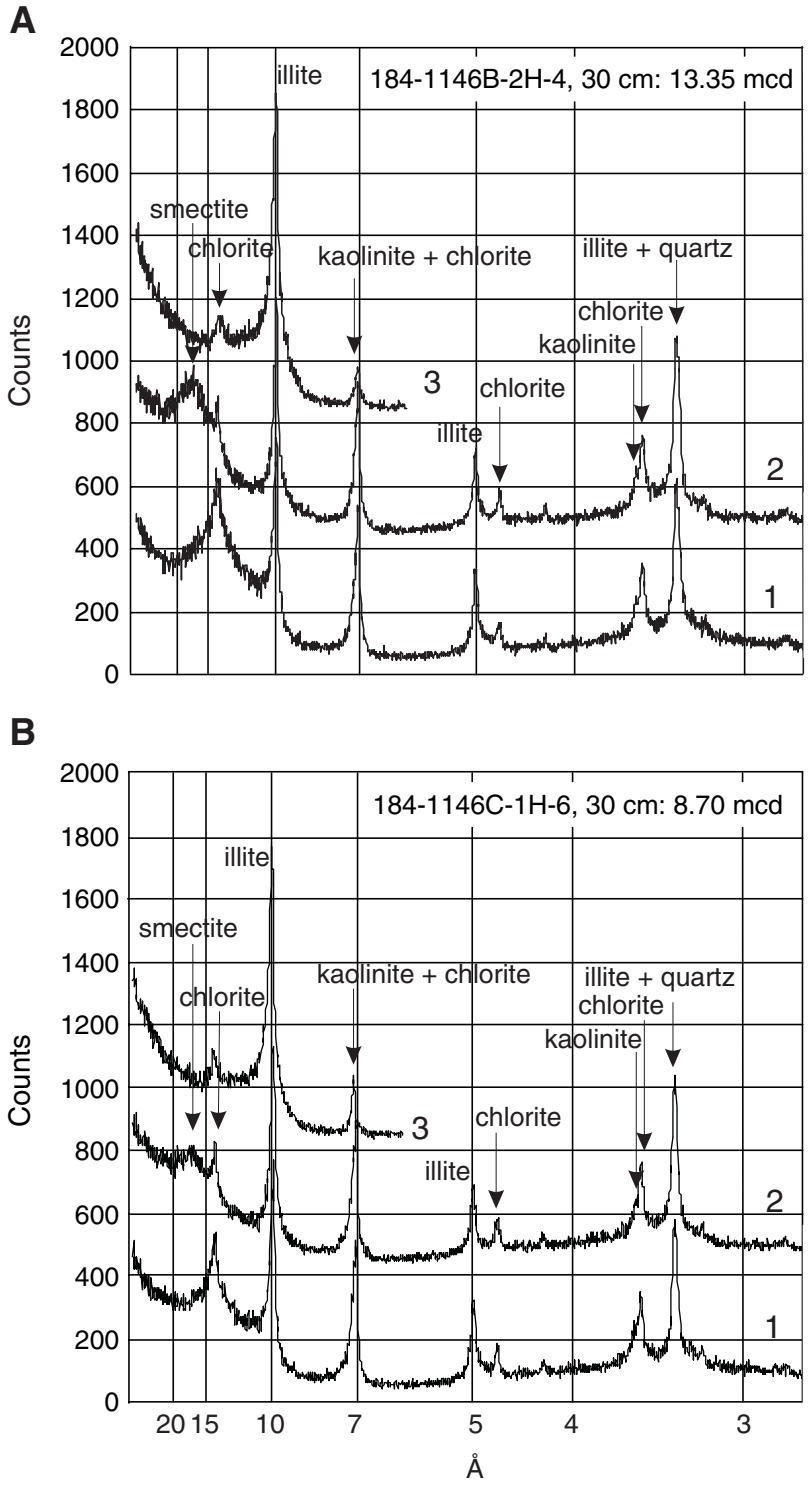

Figure F3. Color reflectance parameter L* and variations of clay-mineral assemblages. Smectite corresponds to smectite and illite-smectite mixed-layer minerals.

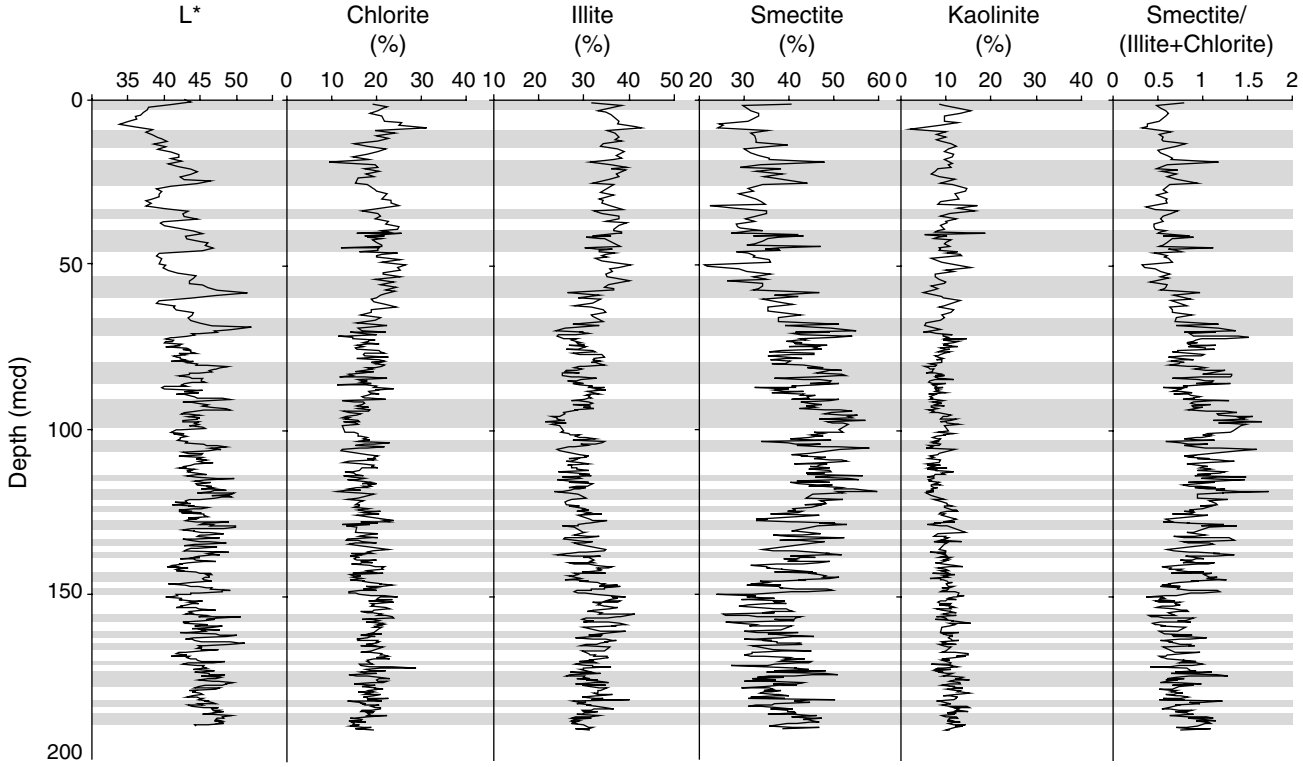

Table T1. Summary of depth and relative abundance of clay-mineral constituents.

Core, section, interval* (cm)	Depth (mcd)	Chlorite (%)	Illite (%)	Kaolinite (%)	Smectite (%)
184-1146B-					
1H-1, 105	1.05	19.2	31.7	8.4	40.7
1H-2, 30	1.80	22.4	38.3	9.6	29.7
1H-2, 105	2.55	21.5	35.6	12.5	30.5
1H-3, 30	3.30	20.2	33.0	15.3	31.5
1H-3, 105	4.05	18.6	34.9	13.2	33.4
1H-4, 30	4.80	21.2	35.9	9.6	33.3
184-1146C-					
1H-4, 105	6.45	21.9	37.6	9.6	30.9
1H-5, 30	7.20	25.7	37.4	12.6	24.3
1H-5, 105	7.95	24.9	41.2	8.7	25.3
1H-6, 30	8.70	31.2	42.6	2.1	24.2
1H-6, 105	9.45	19.7	35.1	9.9	35.3
184-1146B-					
2H-2, 30	10.35	24.1	36.7	7.8	31.4
2H-2, 105	11.10	20.0	37.6	9.9	32.5
2H-3, 30	11.85	22.5	36.9	7.9	32.6
2H-3, 105	12.60	20.3	38.3	8.8	32.5
2H-4, 30	13.35	15.0	34.1	11.0	39.8
2H-4, 105	14.10	17.8	33.7	12.3	36.2
2H-5, 30	14.85	22.1	37.5	10.4	30.0
184-1146C-					
2H-4, 30	15.90	20.3	38.8	9.6	31.4
2H-4, 105	16.65	17.8	37.1	11.7	33.4
2H-5, 30	17.40	14.8	38.5	11.2	35.5
2H-5, 105	18.15	18.2	36.7	9.7	35.4
2H-6, 30	18.90	9.4	31.4	11.3	48.0
2H-6, 105	19.65	19.8	36.1	10.5	33.6
2H-7, 30	20.40	20.3	39.5	11.1	29.2
184-1146B-					
3H-2, 30	20.90	17.2	36.1	8.3	38.4
3H-2, 105	21.65	20.7	39.1	7.6	32.6
3H-3, 30	22.40	17.6	37.1	6.8	38.4
3H-3, 105	23.15	19.3	37.7	8.5	34.5
3H-4, 30	23.90	15.9	35.7	11.9	36.5
3H-5, 30	25.40	15.2	32.0	8.7	44.1
184-1146C-					
3H-4, 30	25.60	17.9	36.4	11.5	34.1
3H-5, 30	27.10	19.7	35.0	14.5	30.8
3H-5, 105	27.85	20.1	33.7	14.2	32.1
3H-6, 30	28.60	22.5	36.5	12.1	28.9
184-1146B-					
4H-1, 105	29.85	21.2	33.4	12.9	32.5
4H-2, 30	30.60	23.3	34.2	8.7	33.8
4H-2, 105	31.35	23.1	34.0	8.2	34.7
4H-3, 30	32.10	25.1	35.6	16.8	22.5
4H-3, 105	32.85	21.0	38.5	12.5	27.9
4H-4, 30	33.60	16.7	32.2	16.3	34.9
4H-4, 105	34.35	20.3	33.8	10.8	35.0
4H-5, 30	35.10	20.9	37.8	8.8	32.5
184-1146C-					
4H-3, 105	36.00	19.8	37.8	12.2	30.2
4H-4, 30	36.75	22.6	34.9	10.0	32.5
4H-4, 105	37.50	22.0	39.5	10.3	28.1
4H-5, 30	38.25	25.0	37.7	8.8	28.5
4H-5, 105	39.00	24.7	36.6	9.7	29.0
184-1146B-					
5H-1, 30	39.60	21.1	36.6	8.3	34.0
184-1146C-					
4H-6, 30	39.75	22.5	38.2	7.4	31.8
184-1146B-					
5H-2, 105	40.35	15.7	38.5	18.8	27.1
184-1146C-					
4H-6, 105	40.50	25.5	37.4	5.4	31.7
184-1146B-					
5H-2, 30	41.10	17.4	31.9	8.6	42.1
184-1146C-					
4H-7, 30	41.25	21.7	36.1	10.2	32.0
5H-1, 30	41.50	18.0	30.5	8.1	43.4
184-1146B-					
5H-2, 105	41.85	21.1	33.7	7.4	37.7
184-1146C-					
5H-1, 105	42.25	19.2	34.4	11.1	35.2
5H-2, 30	43.00	20.1	35.8	10.1	34.0
5H-2, 105	43.75	21.3	36.9	9.6	32.3
184-1146B-					
5H-4, 30	44.10	21.2	38.1	10.3	30.5
184-1146C-					
5H-3, 30	44.50	12.0	30.1	10.7	47.1
184-1146B-					
5H-4, 105	44.85	20.7	33.1	8.3	37.9
184-1146C-					
5H-3, 105	45.25	20.4	36.3	8.7	34.6
184-1146B-					
5H-5, 30	45.60	20.3	33.4	8.6	37.7
184-1146C-					
5H-4, 30	46.00	16.3	33.3	12.5	37.9
184-1146B-					
5H-5, 105	46.35	24.7	36.9	10.2	28.2
184-1146C-					
5H-4, 105	46.75	21.3	34.8	13.1	30.9
184-1146C-					
5H-6, 30	47.10	20.0	34.0	13.5	32.5
184-1146C-					
5H-5, 30	47.50	20.1	35.0	12.9	32.0
5H-5, 105	48.25	25.2	32.4	6.8	35.5
5H-6, 30	49.00	21.2	33.8	9.1	36.0
184-1146B-					
6H-1, 105	49.75	26.3	40.2	12.1	21.3
6H-2, 30	50.50	24.8	37.7	15.6	21.9
6H-2, 105	51.25	25.3	35.8	10.1	28.9
6H-3, 30	52.00	21.4	36.3	11.7	30.7
6H-3, 105	52.75	21.5	34.9	7.6	36.0
6H-4, 30	53.50	25.3	35.0	7.6	32.1
6H-4, 105	54.25	19.7	36.9	8.4	35.0
6H-5, 30	55.00	23.7	40.2	10.0	26.1
6H-5, 105	55.75	20.9	35.3	9.6	34.2
6H-6, 30	56.50	24.3	34.7	6.8	34.3
6H-6, 105	57.25	22.0	36.6	8.2	33.2
184-1146C-					
6H-5, 30	57.65	24.1	36.6	7.2	32.0
6H-5, 105	58.40	21.7	26.5	4.9	46.9
6H-6, 30	59.15	21.0	33.3	9.0	36.8
6H-6, 105	59.90	19.9	28.7	9.3	42.1
184-1146B-					
7H-2, 30	60.60	18.8	33.7	13.3	34.2
7H-2, 105	61.35	19.3	32.0	11.4	37.3
7H-3, 30	62.10	21.9	27.7	9.5	40.9
7H-3, 105	62.85	24.5	31.6	8.6	35.4
7H-4, 30	63.60	18.8	34.2	11.8	35.2

Notes: Clay mineral content corresponds to semiquantitative data, based on the measurement of the surface of the basal reflection on the ethylene glycol XRD diagram. Smectite content combines smectite and illite-smectite mixed-layer minerals. * = all intervals are 2 cm long, and the top of each interval is given. Only a portion of this table appears here. The complete table is available in **ASCII.**